Science in China Series E: Technological Sciences

www.scichina.com
tech.scichina.com
www.springerlink.com

Experimental investigation and analysis on flexural performance of functionally graded composite beam crack-controlled by ultrahigh toughness cementitious composites

LI QingHua & XU ShiLang†

State Key Laboratory of Coastal and Offshore Engineering, Dalian University of Technology, Dalian 116024, China

Based on the concept of functionally graded concrete, UHTCC (ultrahigh toughness cementitious composites) material with excellent crack-controlling ability is strategically substituted for part of the concrete, which surrounds the main longitudinal reinforcement in a reinforced concrete member. Investigations on bending behavior of such a functionally graded composite beam crack-controlled by UHTCC (abbreviated as UHTCC-FGC beam) have been carried out. After establishing a theoretical calculation model, the paper discusses the results of four-point bending experiment on long composite beams without web reinforcement, and validates the theoretical formulae through experimental results of UHTCC-FGC beams with different thicknesses of UHTCC layer. Besides improving bearing capacity and saving steel reinforcements, the results indicate that UHTCC-FGC beams can also effectively control the deformation and enhance the ductility of members. At last, the optimal thickness of UHTCC layer in UHTCC-FGC beams has been confirmed, which can not only save materials and improve mechanical performance of members, but also be very effective in preventing corrosion-induced damage and enhancing the durability of members by controlling crack width below 0.05 mm under service conditions.

UHTCC, crack control, functionally graded, experimental research, validation, durability

On the basis of micromechanical principles and fracture mechanics, Li and Leung[1] proposed the mechanism of crack bridging for random oriented short fiber reinforced cementitious composite (RSFRCC for short). To achieve the strain hardening behavior, the first crack stress criterion and steady state cracking criterion were established as guidelines to optimize material micromechanical parameters[2,3]. After carefully tailoring the fiber, matrix, and fiber/matrix interface microstructures, the strain hardening ECC (engineered cementitious composite) was successfully designed with a moderately low fraction of discontinuous short-cut fibers in the laboratory[4]. Subsequently, UHPFRCC (ultrahigh performance fiber reinforced cementitious composites) was developed in Japan. In recent years, the material was made in China too, which was named as UHTCC (ultrahigh toughness cementitious composites) mainly considering the excellent toughness of the material and for the convenience of engineers to understand and apply[5]. This kind of composite material displays strain hardening behavior with tensile strain capacity in excess of 3% in uniaxial tension under the condition of low fiber (mainly PVA or PE fiber) volume fraction. Steady state cracking mode and multiple fine cracks are the typical features

Received January 22, 2009; accepted March 11, 2009
doi: 10.1007/s11431-009-0161-x
†Corresponding author (email: slxu@dlut.edu.cn)
Supported by the Key Program of the National Natural Science Foundation of China (Grant No. 50438010) and the Research and Application Programs of Key Technologies for Major Constructions in the South-North Water Transfer Project Construction in China (Grant No. JGZXJJ2006-13)

of UHTCC under uniaxial tension load. And the crack width can be still kept at a low level below 100 μm, even corresponding to ultimate tension strain. What is worthy to note is that this steady state crack width is an intrinsic material property of UHTCC material and independent of applied load, and size and geometry of UHTCC components. The obvious strain hardening behavior of UHTCC under tension or bending load[6,7] ensures load will not decrease suddenly after cracking. Prominent toughness and excellent crack-dispersion capacity make the material have tremendous potential in seismic strengthening and rehabilitation applications, and be considered as a potential structural material where long-term durability must be maintained.

Development of UHTCC has involved numerous laboratory tests, analytical and numerical investigations to establish fundamental characteristics, and additional tests to verify the performance of components made of this composite material. In recent decades, a variety of applications of this material were developed very fast in America, European and Japan, ranging from repair and retrofit of structures to precast structural elements requiring high ductility. An American concrete bridge deck patch was performed in 2005. After 4 months of winter exposure, the concrete crack observed shortly after casting was widened to 2 mm, and sections of the concrete patch were severely deteriorating after 10 months; while no visible cracking occurred within the UHTCC patch shortly after patching, and after 4 months of winter exposure, even 30 months after patching, only a number of small microcracks, each about 50 μm wide, were found within the UHTCC[8]. In 2005, UHTCC material was successfully used in building a tunnel passing entirely under the main Swiss Zurich railway station with 50% less time and 30% less cost, and corrosion caused by the electrolysis of reinforced concrete structures was prevented[9]. Also, UHTCC has had abroad application in Japan. Because of the processing flexibility, the material was used for surface repair of Mitaka-Dam[10], irrigation channels[11], retaining walls[12], and railway viaducts[13] by direct spraying method, providing new material and repairing technology to improve ductility of old structures. Mihara Bridge in Hokkaido, which was open to traffic in 2005, adopted composite UHTCC——steel deck for stiffening deck to decrease stress in deck steel with 40% weight reduction and 50% cost reduction[14]. At the same time, UHTCC members were incorporated as coupling beam dampers into high-rise reinforced concrete buildings in Japan by taking advantage of the excellent energy-absorbing ability of UHTCC under alternate loading[15]. And this provides a potential material for seismic resistant. Moreover, textile and UHTCC were used together by making use of the outstanding crack-controlling ability of UHTCC[16], providing a new choice of material in high-rise and large-span structures, and handling problems about maintaining and strengthening of reinforced concrete structures under exposure environment.

It is recognized that uncracked protection cover is nearly impermeable and adequately protects reinforcements from surface exposure and corrosives[8]. Emergence of wide cracks has been considered as a main reason for a great loss of durability and reduction of service life[17] for the ordinary reinforced concrete structures. Far back to ancient China, organic matters and inorganic matters were already used together to improve the toughness of materials to restrain crack opening[18]. At the present time, an exact limitation of crack width is often guided in some design codes for requirement of durability of structures. However, the limitation of crack width required for durability for some important structures under aggressive environment is too strict for ordinary reinforced concrete structures to achieve. Taking advantages of the superior mechanical properties and multiple cracking mode of UHTCC, Maalej and Li[19] firstly proposed the concept of FGC beam through an experimental investigation on flexural performance of a single reinforced concrete member. In their study, UHTCC was used as a replacement for the concrete material that surrounds the longitudinal reinforcements. In a later study by Maalej et al.[20], the accelerated corrosion experiment was performed on FGC beams. However, necessary knowledge about the determination of the optimal UHTCC layer thickness and theoretical design method of UHTCC-FGC members were not dealt with. Therefore, research work relating to mechanical performance of UHTCC-FGC flexural members was in progress. Subsequent to theoretical analysis[21], a four-point bending experiment was carried out in the paper to validate the theoretical model. By employing excellent crack-control ability of UHTCC, UHTCC layers with different thicknesses were strategically substituted for part of concrete material surrounding the longitudinal reinforcement. Crack propagation of UHTCC-FGC

beams was carefully observed during the whole flexural loading process. Then comparison of load carrying capacity and ductility between UHTCC-FGC beams and reference reinforced concrete beams, and discussion on the optimal thickness of UHTCC layer were presented subsequently.

1 Experimental programs

1.1 Materials

Two performance requirements were imposed on the UHTCC material to replace concrete to serve its intended purpose[19]. Firstly, the strain at the extreme edge of the tensile zone must be less than the ultimate tensile strain capacity of UHTCC, to avoid macro cracks due to strain localization in the UHTCC layer. Secondly, the ultimate crack width of UHTCC should be less than the allowable crack width under a particular environment. According to the 2005 revised edition of "Design and Construction Direction to Concrete Structure Durability" (CCES01-2004) in China, the crack width for ordinary reinforced concrete structures exposed in severe environment should be limited to 0.1 mm[22]. In consideration of long-term environmental effects, crack width of practical structures is higher than that of tested specimens in the laboratory. Therefore, the UHTCC material used in the experiment should provide a sufficiently high cracking strength as well as small crack width at ultimate tensile strain capacity. For the purpose of this investigation, an UHTCC composite material with 2% (volume fraction) PVA fiber was selected to substitute for concrete as protection layer of longitudinal reinforcements. This composite material exhibits a strain hardening behavior and a saturated multiple cracking feature under uniaxial tension load (see Figures 1 and 2)[5]. As Figure 2 indicates, the ultimate tensile strain capacity of this composite material was higher than 4%, and the maximum crack width at ultimate tensile strain capacity measured in experiments satisfied the requirement established for the UHTCC protection layer.

Figure 1 Saturated multiple cracking of UHTCC under uniaxial tension.

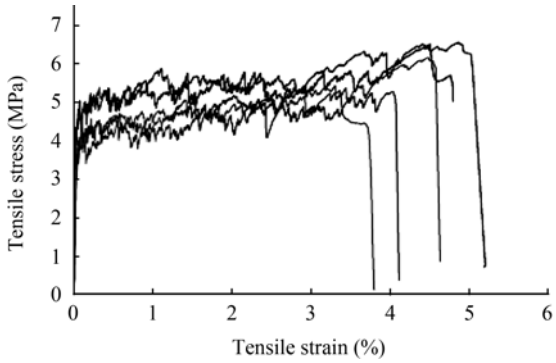

Figure 2 Uniaxial tensile stress versus strain curves of UHTCC.

The UHTCC material consisted of cementitious binder, fine sand, water, fiber and superplasticizer without coarse aggregate. The fiber used was KURALON K-II REC15 PVA fiber with corresponding properties given in Table 1.

Three ordinary reinforced concrete beams with the same reinforcement ratio were also prepared as reference specimens to the UHTCC-FGC beams under the same bending load condition. For concrete material, the mix proportion (in unit of kg/m^3) is water: cement: fly ash: coarse aggregate: sand = 276∶538∶231∶677∶677. Type I Portland cement, Grade I fly ash and river sand were used. Coarse aggregate was crush lime stone with the size of 5—10 mm. Superplasticizer was also added to improve workability of the concrete mixture.

1.2 Specimen preparation

In this research, the long beams without web reinforcement, which had a 120 mm×80 mm rectangular cross section and a 2000 mm length, were designed to ensure flexural failure mode with the configuration given in Figure 3. The cover thickness distance from the extreme tensile fiber to the sheath of reinforcement was 20 mm. The longitudinal reinforcement consisted of an HRB335 bar, corresponding to a reinforcement ratio of 1.18%.

Four groups of UHTCC-FGC beams with different thicknesses of UHTCC layer were prepared during the experiment (Figure 4). The serial numbers UHTCC50, UHTCC35, UHTCC 25 and UHTCC15 stand for specimens with 50, 35, 25 and 15 mm UHTCC layers, respectively. For UHTCC50, the cross section UHTCC layer had the same centroid with longitudinal reinforcement; for UHTCC35, the thickness of UHTCC layer was selected such that UHTCC layer just overlaid longitudinal reinforcement; for UHTCC25, the interface between concrete layer and UHTCC layer was just at the centroid

Table 1 Properties of PVA fiber

Type	Length (mm)	Diameter (μm)	Tensile strength (MPa)	Elongation (%)	Tensile modulus (GPa)	Density (g/cm^3)
KURALON K-II REC15	12	39	1620	7	42.8	1.3

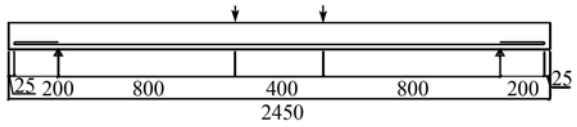

Figure 3 Sketch of beam.

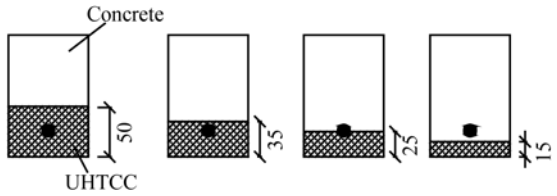

Figure 4 Cross sections of UHTCC-FGC beams.

of longitudinal reinforcement; for UHTCC15, the whole UHTCC layer was used as protection cover and longitudinal reinforcement was embedded in the concrete layer. Moreover, a group of ordinary reinforced concrete beams RC12 with the same reinforcement ratio of UHTCC-FGC beams was designed as reference specimens.

A pair of electric resistance strain gauges of 2 mm in length was symmetrically fixed on the surface of steel reinforcement at the pure bending part. Then reinforcements were fixed in rectangular wood molds before casting. To avoid the subsidence of coarse aggregates into UHTCC, fresh concrete was mixed and cast firstly with the required thickness. During the mixing process of UHTCC, the cementitious binders and fine sand were first put into a Hobart A200 type mixer and mixed for about 2 min in dry state. Then water and superplasticizer were added in sequence. Until the mixture presented good workability, PVA fiber was added by keeping a constant mixing speed. When the fresh composites were touched with hand, no fiber balls were found to indicate the fibers are uniformly dispersed into the mortar. UHTCC layer should be cast about an hour later after concrete layer to avoid debonding of the two layers and prevent the coarse aggregate in concrete from entering the UHTCC layer. Each layer was vibrated for several minutes by an immersible concrete vibrator. After casting, all the specimens were covered with plastic sheets to avoid evaporation and demolded after 48 h. Then specimens were cured outdoors with water spray once a day.

1.3 Testing procedure

The schematic picture of test setup is shown in Figure 5. Two displacement transducers were fixed at both sides of the middle span to measure the deflection, and two linear variable differential transformers (LVDT) were fixed at the location of support to measure support displacement. On the top and bottom surfaces of specimens at the center span, a pair of LVDTs was attached to measure the maximum compressive and tensile deformation in a 320 mm gage respectively, and an LVDT fixed at the location of steel bar was used to measure tension strain of UHTCC or concrete at the same level of steel bar. According to the theoretical model, first-cracking of UHTCC-FGC beams can occur either in concrete layer or in UHTCC layer. Six electric resistance strain gauges of 50 mm in length were connected with the way of full-bridge circuits and fixed continuously at the bottom of the beams to determine the first cracking occurrence of UHTCC layer; four electric resistance strain gauges of 100 mm in length were connected with the way of half-bridge circuits and fixed

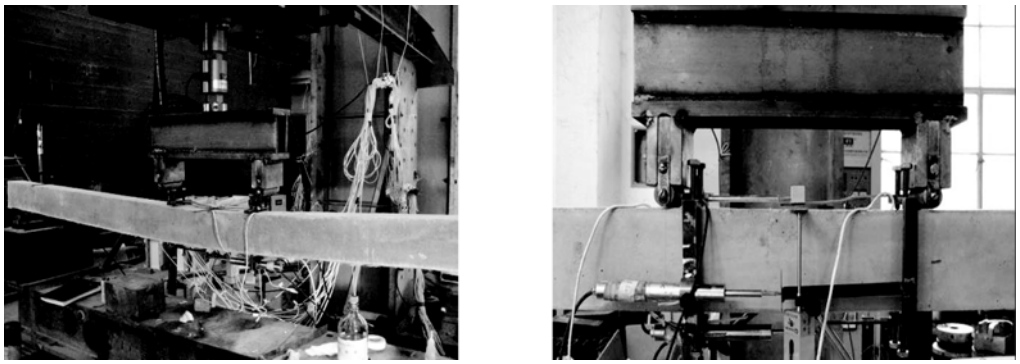

Figure 5 Pictures of test setup.

continuously above the interface of the two layers to observe the first cracking occurrence of concrete layer. The MTS testing system with the maximum capability of 1000 kN was used to perform the test. In addition, the plots of load versus displacement of mid-span were monitored during the experiments under control of displacement with a constant rate of 0.5 mm/min. During the process, a crack width measurement instrument with a 40× lens was used to monitor the development of crack.

2 Experimental results and discussion

2.1 Moment-curvature and load-deflection relationship

2.1.1 Experimental curves. Figure 6 shows the experimental moment vs. curvature and load vs. deflection relations for each group. Notice that not all of the specimens were loaded to final failure, yet some were stopped loading when the dominating crack of width more than 0.1 mm appeared. From the figure, it can be found that the moment-curvature and load-deflection relation curves of the UHTCC-FGC beams are similar to the curves of ordinary reinforced concrete beams. For all specimens tested, the first-cracking loads were close and the curves behaved linearly before cracking. Although the UHTCC-FGC beam has cracked, considering high tensile load-bearing capacity with prominent tensile strain capacity of UHTCC in unaxial tension, UHTCC layer in tension zone continues to be able to undertake tension load. The stiffness of the UHTCC-FGC beam is somewhat weakened because the beam is cracked, resulting in a turning point in the curve of moment-curvature relationship. Curvature of section increases abruptly once the steel reinforcement yields, which is indicated in moment-curvature curves by the second obvious turning point, and meanwhile the UHTCC-FGC beam enters the failure stage. The moment almost ceases to increase with deflection, so that the moment-curvature curve is nearly horizontal.

2.1.2 Comparison between test and calculated results. During establishing the theoretical calculation model of the UHTCC-FGC flexural member[21], the whole bending process were divided into three distinct stages, namely, the elastic stage before the matrix cracks, the service stage starting from appearance of the first crack till the elastic limit stress of steel reinforcement is reached, and the failure stage beginning with the yielding of steel reinforcement and ending in the failure of the beam. Based on mechanical models of materials and a series of assumptions, i.e., plane section assumption, compatible deformation between steel reinforcement and matrix, adequate bond between concrete and UHTCC as well as effectivity of UHTCC in tensile zone after cracking, a calculation model of UHTCC-FGC flexural members was detailedly presented by two equilibrium equations of force and moment for the beam section. The calculation formulae of moment at each stage are as follows.

(a) Elastic stage

$$M = bf_c\frac{\varepsilon_t}{\varepsilon_0}\left(\frac{2h^3}{3c} - h^2 + \frac{c^2}{3}\right) - bf_c\frac{\varepsilon_t^2}{\varepsilon_0^2}\left(\frac{h^4}{4c^2} - \frac{2h^3}{3c} + \frac{h^2}{2} - \frac{c^2}{12}\right)$$
$$- b\frac{\sigma_{tc}}{\varepsilon_{tc}}\varepsilon_t\left(\frac{t^2}{2} - \frac{t^3}{3c}\right) - b\frac{f_t}{\varepsilon_{tu\text{-}con}}\varepsilon_t\left(\frac{c^2}{6} - \frac{t^2}{2} + \frac{t^3}{3c}\right)$$
$$- \frac{c-m}{c}\varepsilon_t E_s A_s m. \quad (1)$$

(b) Service stage with cracks

After both concrete layer and UHTCC layer crack, there are two cases of stress and strain condition.

When the concrete in compressive zone still behaves linearly, namely $\varepsilon_c < \varepsilon_0$:

$$M = bf_c\frac{\varepsilon_t}{\varepsilon_0}\left(\frac{2h^3}{3c} - h^2 + \frac{c^2}{3}\right) - bf_c\frac{\varepsilon_t^2}{\varepsilon_0^2}\left(\frac{h^4}{4c^2} - \frac{2h^3}{3c} + \frac{h^2}{2} - \frac{c^2}{12}\right)$$
$$- \frac{t^2 b}{2}\frac{\sigma_{tu} - \sigma_{tc}}{\varepsilon_{tu} - \varepsilon_{tc}}(\varepsilon_t - \varepsilon_{tc}) - \frac{t^2 b}{2}\sigma_{tc} + \frac{t^3 b}{3}\frac{\sigma_{tu} - \sigma_{tc}}{\varepsilon_{tu} - \varepsilon_{tc}}\frac{\varepsilon_t}{c}$$
$$- \frac{c-m}{c}\varepsilon_t E_s A_s m. \quad (2)$$

When the maximum compressive strain of concrete satisfies $\varepsilon_0 \leqslant \varepsilon_c < \varepsilon_{cu}$:

$$M = \frac{bf_c h^2}{2} - bf_c c^2\left(\frac{\varepsilon_0^2}{12\varepsilon_t^2} + \frac{1}{2} + \frac{\varepsilon_0}{3\varepsilon_t}\right) - \frac{c-m}{c}\varepsilon_t E_s A_s m$$
$$- \frac{t^2 b\sigma_{tc}}{2} + a^2 b\frac{\sigma_{tu} - \sigma_{tc}}{\varepsilon_{tu} - \varepsilon_{tc}}\left(\frac{t\varepsilon_t}{3c} - \frac{\varepsilon_t}{2} + \frac{\varepsilon_{tc}}{2}\right). \quad (3)$$

(c) Failure stage after steel yielding

$$M = \frac{bf_c h^2}{2} - bf_c c^2\left(\frac{\varepsilon_0}{3\varepsilon_t} + \frac{\varepsilon_0^2}{12\varepsilon_t^2} + \frac{1}{2}\right) - f_y A_s m - \frac{t^2 b}{2}\sigma_{tc}$$
$$+ \frac{\sigma_{tu} - \sigma_{tc}}{\varepsilon_{tu} - \varepsilon_{tc}}\left(\frac{t^3 b\varepsilon_t}{3c} - \frac{t^2 b(\varepsilon_t - \varepsilon_{tc})}{2}\right). \quad (4)$$

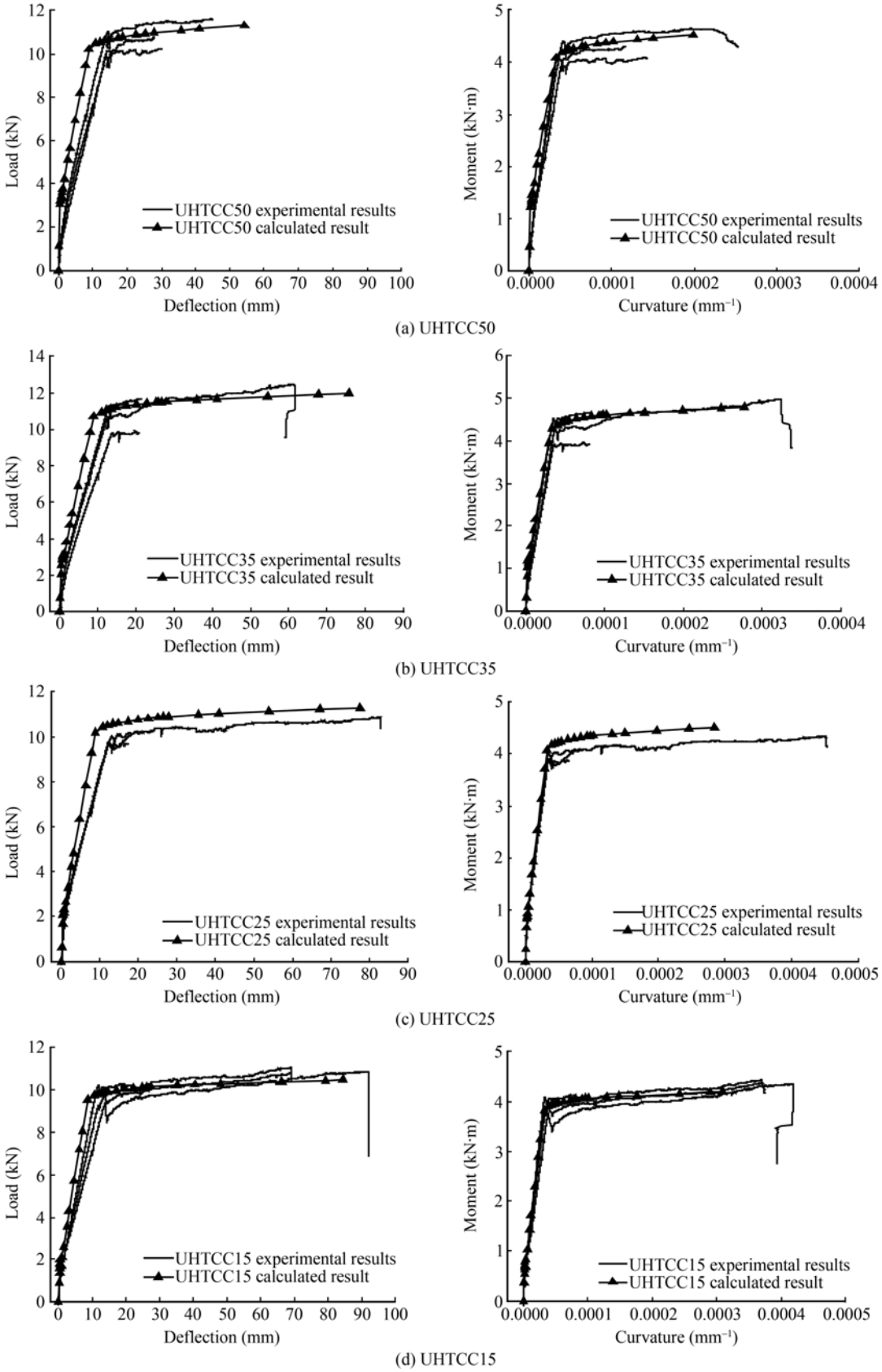

Figure 6 Comparison between experimental and calculated results of UHTCC-FGC beams.

Curvature of a section can be expressed as

$$\varphi = \frac{1}{\rho} = \frac{\varepsilon_t}{c}. \quad (5)$$

The maximum mid-span deflection for a UHTCC-FGC beam is given by

$$f = S\frac{L^2}{\rho} = S\frac{\varepsilon_t}{c}L^2. \quad (6)$$

The symbols in the above expressions denote respectively σ_{tc} = first-cracking tensile strength of UHTCC, ε_{tc} = first-cracking tensile strain of UHTCC, σ_{tu} = ultimate tensile strength of UHTCC, ε_{tu} = ultimate tensile strain of UHTCC, f_y = yielding stress of steel reinforcement, ε_y = yielding strain of steel reinforcement, A_s = section area of steel reinforcement, ε_{tu-con} = ultimate tensile strain of concrete, f_t = ultimate tensile stress of concrete, f_c = axial compressive strength of concrete, h = depth of beam section, b = width of beam section, t = thickness of UHTCC layer, m = distance from the extreme tensile fiber to the centroid of reinforcement, c = distance from the extreme tensile fiber to the neutral axis, ε_t = strain of UHTCC at the extreme edge of the tension zone, S = the deflection coefficient related with the form of the load, and supporting condition, L = effective span.

By inputting parameters of the materials[21] and the dimensions of beams into the calculation formulae, the moment-curvature curves of UHTCC-FGC beams are analytically obtained and presented in Figure 6 in comparison to the test results. As Figure 6 and Table 2 indicated, all tested beams underwent three stages as above mentioned and failed in the tension-compression failure mode which is consistent with theoretical prediction. There is a reasonable agreement between the calculated and the test results, especially both moment and curvature presented little difference before yielding. This suggests that the theoretical model can be used to predict the flexural performance of UHTCC-FGC beams at different stages. But the calculated maximum deflection is smaller than the test result, because of the neglect of slip between UHTCC and concrete and slip between steel and matrix. For UHTCC25 specimens, the adhesive interface failure took place between UHTCC layer and concrete layer, resulting in a lower load-bearing capacity than the calculated result. Although the test and calculated ductility indices of UHTCC50 are almost the same, it can be seen from Table 2 that the two test ductility indices of the other UHTCC-FGC beams are higher than the calculated values. The ductility indices calculated by theoretical formulae are conservative, but they are rational to predict ductility of structures or members in practice.

2.1.3 Comparison between UHTCC-FGC and reinforced concrete beams. Comparison of moment-curvature and load-deflection relationships between UHTCC-FGC and reinforced concrete specimens can be concluded

Table 2 Load bearing capacity, deflection and ductility of UHTCC-FGC beams at yielding and ultimate states

Specimens	P_y (kN)	f_y (mm)	φ_y (mm^{-1})	P_u (kN)	f_u (mm)	φ_u (mm^{-1})	Ductility index	
							$\varphi_u-\varphi_y$	φ_u/φ_y
UHTCC50-2	10.19	13.8	$3.2\times^{-5}$	-	-	-	-	-
UHTCC50-3	9.9	13.67	$3.9\times^{-5}$	-	-	-	-	-
UHTCC50-4	11.0	14.2	$3.8\times^{-5}$	11.6	45.4	$2.18\times^{-4}$	$1.8\times^{-4}$	5.74
Calculated results of UHTCC50	10.20	8.87	$3.25\times^{-5}$	11.29	54.30	$1.99\times^{-4}$	$1.66\times^{-4}$	6.12
UHTCC35-2	9.76	14.2	$3.6\times^{-5}$	-	-	-	-	-
UHTCC35-3	10.72	12.89	$3.5\times^{-5}$	12.52	60.9	$3.3\times^{-4}$	$2.95\times^{-4}$	9.43
UHTCC35-4	11.31	12.77	$3.52\times^{-5}$	-	-	-	-	-
Calculated results of UHTCC35	10.71	8.93	$4.28\times^{-5}$	11.90	67.81	$2.48\times^{-4}$	$2.052\times^{-4}$	5.79
UHTCC25-1	10.05	12.4	$3.3\times^{-5}$	10.91	81.66	$4.48\times^{-4}$	$4.15\times^{-4}$	13.58
UHTCC25-2	9.79	12.02	$3.4\times^{-5}$	-	-	-	-	-
UHTCC25-4	9.85	12.34	$3.33\times^{-5}$	-	-	-	-	-
Calculated results of UHTCC25	10.17	8.82	$3.23\times^{-5}$	11.27	77.58	$2.84\times^{-4}$	$2.517\times^{-4}$	8.79
UHTCC15-1	10.01	11.45	$3.3\times^{-5}$	11.19	68.8	$3.68\times^{-4}$	$3.35\times^{-4}$	11.15
UHTCC15-2	9.35	13.54	$3.9\times^{-5}$	10.96	87.88	$4.4\times^{-4}$	$4.01\times^{-4}$	11.28
UHTCC15-3	9.68	13.42	$3.37\times^{-5}$	11.05	69.7	$3.62\times^{-4}$	$3.283\times^{-4}$	10.74
Calculated results of UHTCC15	9.53	8.72	$3.19\times^{-5}$	10.44	79.29	$2.9\times^{-4}$	$2.58\times^{-4}$	9.09
RC12-1	8.825	13.02	$3.59\times^{-5}$	9.75	59.56	$2.25\times^{-4}$	$1.89\times^{-4}$	6.27
RC12-3	8.425	12.90	$3.03\times^{-5}$	9.75	68.9	$1.99\times^{-4}$	$1.40\times^{-4}$	5.61

from Figures 7 and 8. It is found from moment-curvature curves that there is no difference between them before first-cracking and the curves almost overlap after cracking, indicating that the flexural stiffnesses of the specimens are almost the same. It is well known that the flexural stiffness is the product of material elastic modulus and effective moment of inertia. Although the elastic modulus of UHTCC material is only about 2/3 of that of concrete, excellent crack-controlling behavior of UHTCC layer makes the effective moment of inertia of UHTCC-FGC much higher than those of RC12 beams with several wide cracks. From the comparison of deflections shown in Figure 8, it is observed that the yielding deflection of UHTCC-FGC beam is close to that of RC12 beam. On the other hand, due to strain hardening behavior of UHTCC, high load bearing capacity would be obtained by introducing UHTCC into flexural members. Table 2 indicates that the yielding load of each group of UHTCC-FGC beams is 23%, 25.8%, 17.5% and 14.9% higher than that of RC12 beams, respectively. It means that UHTCC can evidently delay the yielding of reinforced steel. When RC12 beam reaches its yielding load, the tested UHTCC-FGC beams are still in the service stage with development of cracks, and present lower deflection than RC12 beams. As a result, improved load bearing capacity, well-controlled deflection and reduced steel products can be realized through the approach to using UHTCC as a replacement for the concrete material.

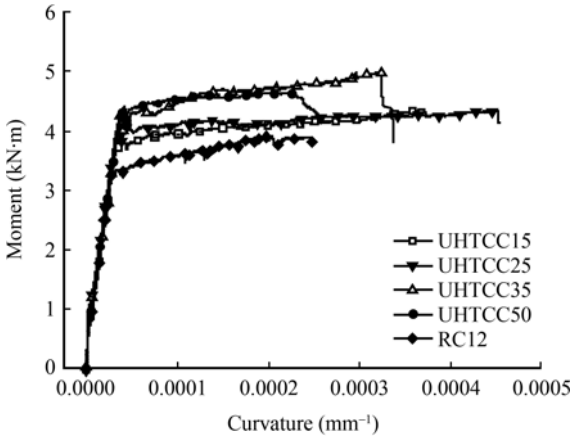

Figure 7 Moment-curvature relationships of UHTCC-FGC and RC beams.

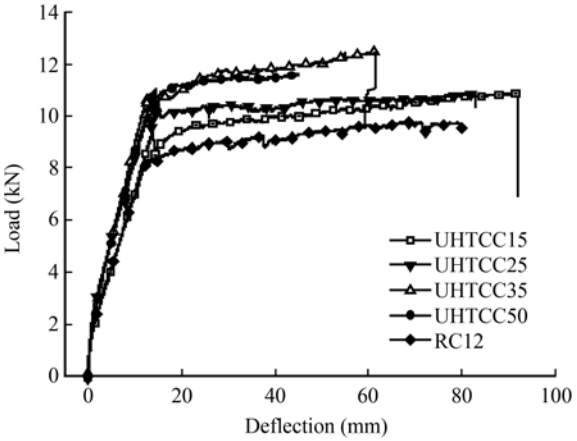

Figure 8 Load-deflection relationships of UHTCC-FGC and RC beams.

Besides satisfying load bearing requirement, a structure or a member is requested to possess high ductility. High ductility enables the members to absorb large amount of strain energy before failure and avoid brittle collapse[23]. So it is highly desirable in structural performance, especially in seismic zone. By comparison of ductility indices ($\varphi_u-\varphi_y$) and φ_u/φ_y shown in Table 2, it is found that except UHTCC50, two ductility indices of other groups of UHTCC-FGC beams are distinctly higher than that of RC12 beams. Whichever the ductility index is compared, ductility of UHTCC-FGC beams is much better than that of ordinary reinforced concrete beams with the same reinforcement ratio.

2.1.4 Influence of the thickness of UHTCC layer. Influence of the thickness of UHTCC layer on load-bearing capacity and deformation can also be concluded through Table 2, Figures 7 and 8. For UHTCC25 specimens, the interface between concrete layer and UHTCC layer was just at the centroid of steel reinforcement, however, serious bond failure took place at the interface of the two layers during the test. Accordingly, this thickness of UHTCC layer adopted is inappropriate to be a replacement of concrete. By comparison between UHTCC50 and UHTCC35, a ultimate moment slightly higher than that of UHTCC50 and far more excellent deformation capacity of UHTCC35 than that of UHTCC50 have been observed obviously. What should be mentioned is that the UHTCC material used in UHTCC35 specimens is 30% less than in UHTCC50. Hence it is not difficult to draw a conclusion that the thickness of UHTCC layer just overlays steel reinforcement is more appropriate for UHTCC-FGC beams. Even for UHTCC15 with just 15 mm thick UHTCC layer, it behaves 10% higher yielding load and much higher ductility capacity than RC12 beams.

2.2 Crack propagation and control of crack width

2.2.1 Determination of first cracking. In the testing,

the occurrence and the location of the first-cracking were indicated by comparison of variations of strain gauges at the bottom and on the side of beams. With the increase of applied load, the first group of cracks (a piece or several pieces of crack) appeared at the weakest location in pure bending zone of the beam. When crack occurred at the range of strain gauge, tensile strain increased suddenly; and when crack occurred out of the range of strain gauge, tensile strain withdrew at once. Determination of first-cracking load and strain via curves of load-strain relation is shown in Figure 9. As mentioned previously[20], if a thick UHTCC layer is designed, first-cracking will happen firstly in the UHTCC layer rather than in concrete layer, such as UHTCC25 (see Figure 9(a)), and the maximum tensile strain of concrete layer keeps an increasing tendency before sud

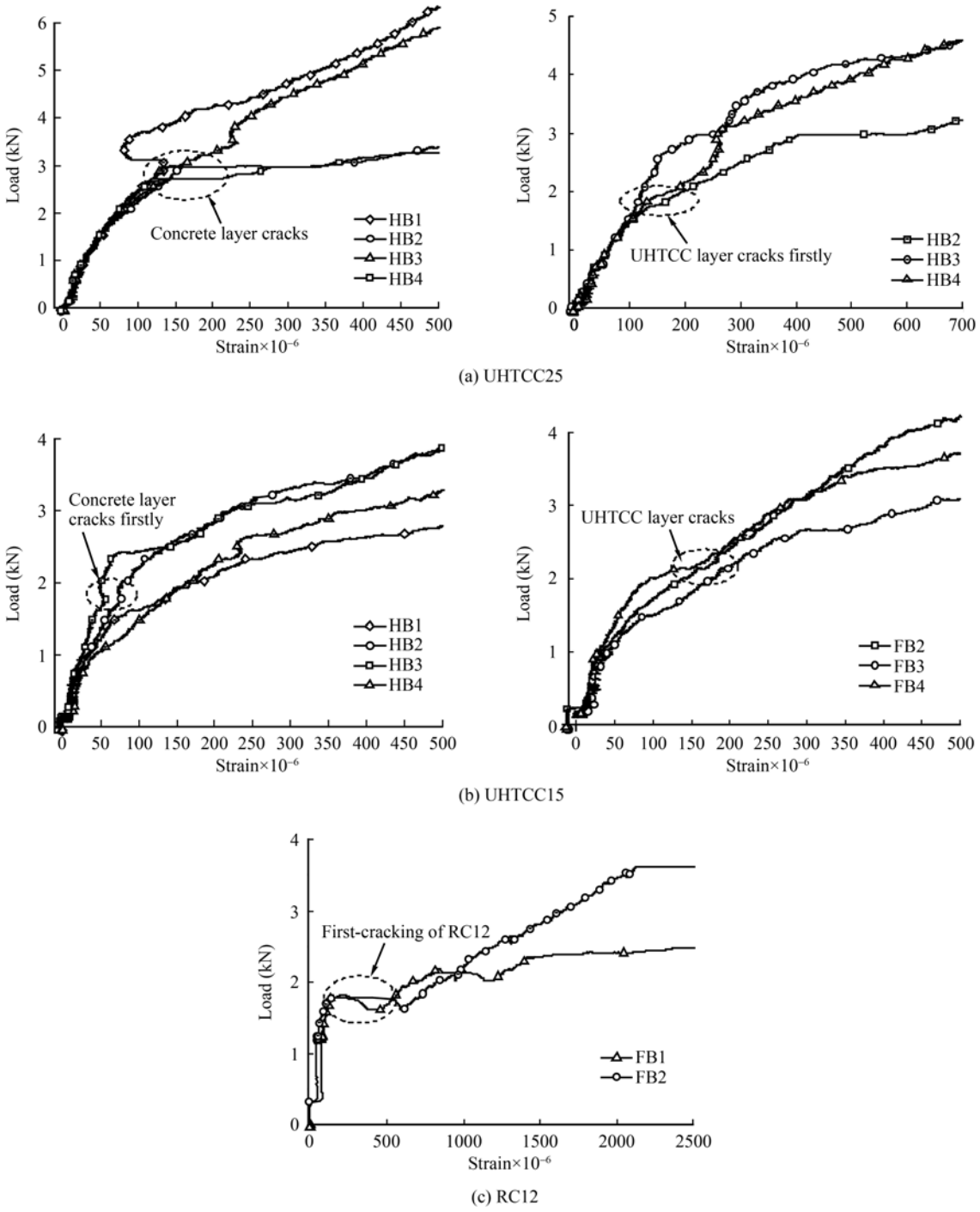

Figure 9 Determination of cracking load.

den variation of tension strain at the bottom of UHTCC layer takes place. On the other hand, if a thin UHTCC layer is designed (such as UHTCC15), when maximum tensile strain of concrete reaches its ultimate tensile strain earlier than that of UHTCC, cracking will happen firstly in concrete layer instead of the UHTCC layer (see Figure 9(b)).

The introduction of flaw made the beams crack prematurely with a low cracking load about 1.6—2.0 kN. When cracks occurs in UHTCC-FGC beams, the increment of strain is far lower than that of reinforced concrete beams (as Figure 9(c) shows), which indicates that crack width of UHTCC-FGC beams is smaller than that of reinforced concrete beams.

2.2.2 Crack width. Under mechanical overloads or environmental loads, cracking is inevitable because of the weakness of concrete such as low tensile strength and strain-softening property after cracking. The injurant such as vapor, carbon dioxide, and chloride may lead to corrosion of steel bar and dramatic reduction of the load bearing capacity once wide cracks have formed in concrete structures[24]. Therefore, an exact limitation of crack width is often guided in some design codes for requirement of durability of structures. For ordinary reinforced structures under different environmental conditions, limitations of crack width have been prescribed in the 2005 revised edition of "Design and Construction Direction to Concrete Structure Durability" (CCES01-2004), in which the allowable maximum crack width is merely 0.1 mm for structures exposed in severe environment[22]. However, it is too strict to achieve for ordinary reinforced concrete structures.

Based on "Code for Design of Concrete Structures" (GBJ50010-2002)[25], the maximum crack width of ordinary reinforced concrete beam with rectangle cross section can be calculated as follows:

$$\omega_{\max} = \alpha_{\mathrm{cr}} \varphi \frac{\sigma_{\mathrm{sk}}}{E_{\mathrm{s}}} \left(1.9c + 0.08 \frac{d_{\mathrm{eq}}}{\rho_{\mathrm{te}}} \right), \tag{7}$$

$$\varphi = 1.1 - 0.65 \frac{f_{\mathrm{tk}}}{\rho_{\mathrm{te}} \sigma_{\mathrm{sk}}}, \tag{8}$$

$$d_{\mathrm{eq}} = \frac{\sum n_i d_i^2}{\sum n_i \nu_i d_i}, \tag{9}$$

$$\rho_{\mathrm{te}} = \frac{A_{\mathrm{s}}}{A_{\mathrm{te}}}, \tag{10}$$

$$\sigma_{\mathrm{sk}} = \frac{M_{\mathrm{k}}}{0.87 h_0 A_{\mathrm{s}}}, \tag{11}$$

where α_{cr} is a coefficient according to load conditions, and it is taken to be 2.1 for reinforced concrete flexural members; φ is a coefficient taking into account the difference among longitudinal reinforcement tension strain, and it is taken to be 0.2 when $\varphi<0.2$ and to be 1 when $\varphi>1$; σ_{sk} is the equivalent steel stress; E_{s} is elastic modulus of steel bar; c is the cover thickness of beam (mm), which is taken to be 20 when $c<20$ and to be 65 when $c>65$; ρ_{te} is the equivalent reinforcement ratio which corresponds to the effective tensile cross-section area of concrete, and when $\rho_{\mathrm{te}}<0.01$ it is taken to be $\rho_{\mathrm{te}}=0.01$; A_{te} is the equivalent section area of concrete in tension zone, which is taken to be $A_{\mathrm{te}}=0.5bh$ for ordinary reinforced concrete beam with rectangle cross-section; A_{s} is the area of non-prestressed longitudinal tension reinforcement; d_{te} is the equivalent diameter of longitudinal tension steel bar (mm); d_i is the diameter of a certain kind of longitudinal tension steel bar (mm); n_i is the number of a certain kind of longitudinal tension steel bar; v_i is a coefficient considering the relative bond property of a certain kind of longitudinal tension steel bar, and it is taken to be 1.0 for non-prestressed ribbed bar; M_{k} is bending moment.

According to the above equations, the reinforcement stress and the corresponding load of RC12-1 in the tests can be calculated by inputting the allowable crack width under different environmental conditions (as Table 3 shows). It is found that when the allowable maximum crack width is limited to be 0.2 mm, the reinforcement stress reaches 75% of the yielding strength; when the allowable maximum crack width is limited to be 0.15 mm, the reinforcement stress is 61.2% of the yielding strength; when the allowable maximum crack width is limited to be 0.1 mm, the reinforcement stress is only 47.6% of the yielding strength. Therefore, for ordinary reinforced concrete members exposed to aggressive environment, the applied load should be restricted to be below 50% of the yielding load to ensure the long-term durability. Therefore, it leads to a great waste of reinforcement.

As mentioned above, UHTCC possesses two important properties, one is the strain hardening behavior which can continuously undertake tension load after first-cracking, especially, it can exceed 3% tension strain

Table 3 The corresponding equivalent steel stresses and loads of the RC beams with different crack width limitations

Crack width (mm)	0.4	0.3	0.2	0.15	0.1	Yielding state of RC12-1
σ_{sk} (MPa)	467.32	368.355	269.39	219.91	170.43	360
M_k (kN·m)	4.6	3.62	2.65	2.16	1.68	3.53

under uniaxial tension, and the other one is the multiple fine cracking characters. Keeping crack width at low level is recognized as an inherent characteristic of UHTCC material, even under the condition of high tensile strain, the average crack width of UHTCC can be controlled as low as below 60 μm (see Figure 10)[8,26]. Investigations[27−29] indicated that the permeability is hardly increased if crack width of concrete is controlled as about 50—60 μm; however, the permeability of ordinary reinforced concrete strictures increases rapidly after cracking. In service stage, the permeability of UHTCC is of several orders of magnitude lower than that of concrete or mortar (as Figure 11 shows). Therefore, the excellent crack-controlling capacity of UHTCC is expected to utilize in concrete structures to improve the durability and service life of structures.

Electric resistance strain gauges and a crack width measurement instrument with a 40× lens were used to monitor the propagation of crack and development of crack width. Figure 12 shows crack pattern of RC12 specimens at failure. For RC12 specimens, the first crack always appeared close to the middle-span of beams. It is seen that a total number of 5 macro cracks appeared in the pure moment zone with the increase of external load applied. The number of cracks ceased to increase after yielding, however just crack width continued extending.

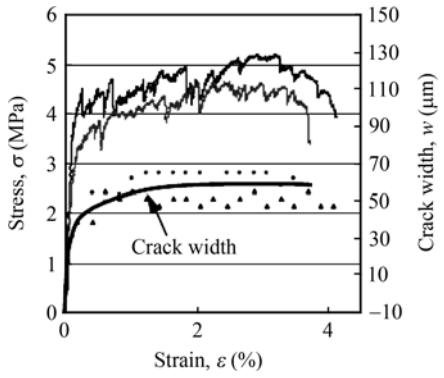

Figure 10 Stress-strain and crack width-strain curves of UHTCC[8].

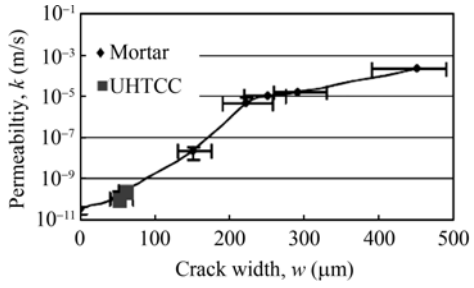

Figure 11 Permeability of UHTCC and mortar after cracking[27].

For UHTCC-FGC beams with first-crack opening in UHTCC layer, the first crack appeared randomly at the weakest location of pure moment region, which could be observed through the variation of electric resistance strain gauges. There was an original bridging stress when crack opening was equal to zero in virtue of fiber/matrix interfacial chemical bond, and the slope of the bridging stress vs. crack opening curve was high[30]. As a result, the bridging stress could resume the level before first-cracking under the condition that only small width of the first crack was needed. Then PVA fibers in UHTCC could provide adequate bridging stress to satisfy the steady state cracking criterion[31]. Load could be transferred from the crack section back to the matrix and cause the formation of another crack, which might initiate from a different matrix defect location. Repetition of this process created the multiple cracking phenomenon. As the applied load increased, concrete layer cracked as soon as the extreme tension fiber of concrete reached its ultimate tensile strength. After the concrete layer cracked and released the tension, the concrete on both sides of the crack tended to shrink away from the crack. But this concentration of concrete was restricted by UHTCC layer until being stopped and the cracks in concrete began to extend downward to the UHTCC layer. By virtue of bond stress between the concrete layer and the UHTCC layer, the tension which was undertaken by concrete would firstly transfer to UHTCC, rather than steel reinforcement. If deformation between reinforcement and UHTCC remained compatible, then stress of steel reinforcement would not increase suddenly by reason of the emergency of fine cracks within the UHTCC layer. Such transfer continued until steel reinforcement yielded. With the increasing applied load, the number of fine cracks in both UHTCC layer and concrete layer increased. Moreover, the cracks in the concrete layer diffused into many fine cracks when they met the UHTCC layer and the opening of cracks in concrete layer was effectively restricted, conforming to the observation in the

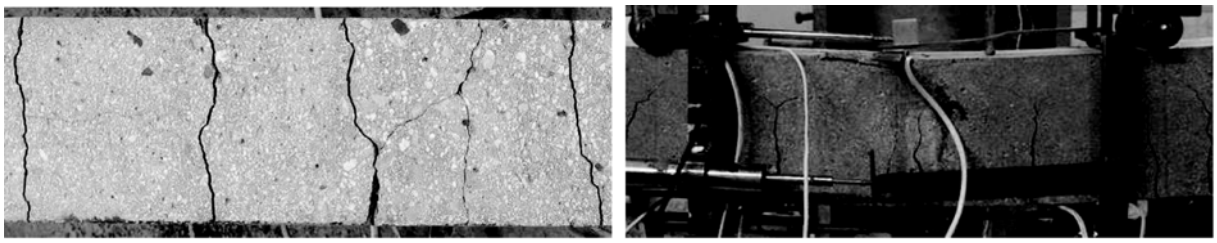

(a) Bottom (b) One side

Figure 12 Crack pattern of RC12 at failure.

study by Maalej and Li[19]. By comparison between the two layers, cracks in UHTCC layer were more difficult to observe without crack width measurement instrument. Different from RC12 specimens, further cracking could be observed in UHTCC layer when the yielding load was approached, although the number of cracks in concrete layer did not increase.

The development of crack opening in UHTCC35 was similar to that in UHTCC50, so only crack pattern of UHTCC50 after failure was given in Figure 13 as an example, where it should be noted that the strain gauge in Figure 13(a) is 50 mm long. Crack patterns of ordinary reinforced concrete beams and UHTCC-FGC beams present an obvious difference. As Figure 12 shows, there were several wide cracks at the bottom of RC12 beams. By contraries, a large amount of fine cracks developed at the bottom of UHTCC-FGC beams (see Figure 13(a)). It is seen from one side of UHTCC-FGC beam that in the concrete layer, a few wide cracks developed; however, in the UHTCC layer, a large amount of fine cracks developed. As Figure 13(b) shows, each wide crack that developed in the concrete layer diffused into many fine cracks when they met the UHTCC layer. Strain concentration took place at these locations where large cracks in concrete layer met the UHTCC material. Stress redistribution would occur because of the bridge effect of PVA fibers in UHTCC material. Accordingly, an expanded zone of matrix cracking developed in the UHTCC layer[19]. Due to shearing stress between the two layers, the corresponding fine cracks to each dominating crack were rootlike. Compared with ordinary reinforced concrete beams, crack width in concrete layer of UHTCC-FGC beams was effectively controlled. It can be concluded that the introduction of the UHTCC layer brought a positive effect on crack-controlling, not only in the UHTCC layer itself but also in the concrete layer.

Delamination between the concrete and the UHTCC layer of UHTCC25 specimens was observed during the test (see Figure 14). The injurant may lead to the corrosion of steel bar through the longitudinal cracks between two layers during its service stage. From moment-curvature curves, a practical ultimate load of this group, distinctly lower than the theoretical value, can also be found as a result of delamination. Accordingly, considering either load bearing capacity or durability, the kind of UHTCC-FGC members, in which the interface between concrete layer and UHTCC layer is just at the centroid of longitudinal reinforcement, is regarded to be inappropriate in practical structures.

For UHTCC15 specimens, the UHTCC layer was used as protection cover and steel reinforcement was embedded in concrete layer. First-cracking occurred in concrete layer, while cracks in UHTCC layer developed mainly through the extension of cracks in concrete ma

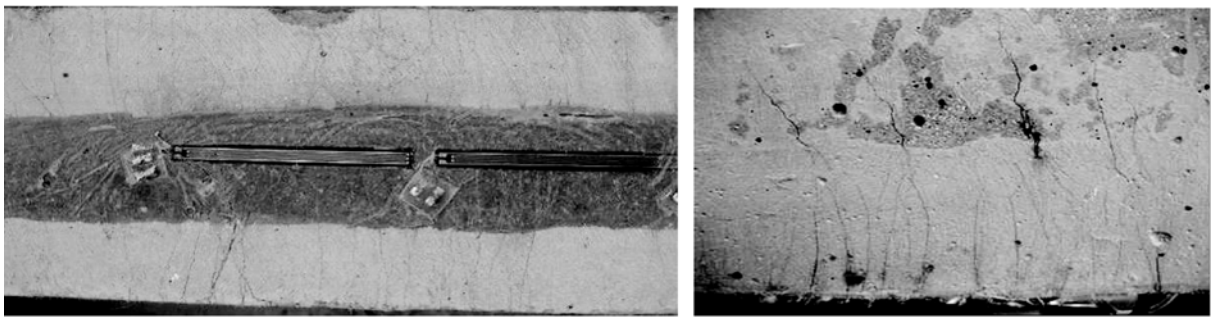

(a) Bottom (b) One side

Figure 13 Crack pattern of UHTCC50 at failure.

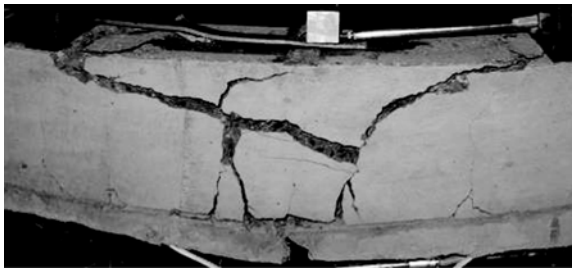

Figure 14 Crack pattern of UHTCC25 at failure.

terial. The number of cracks in UHTCC15 was fewer than those of specimens with thick UHTCC layer (for which UHTCC layer cracks first). However, far lower crack width and much more crack number were still observed in UHTCC15 than in reference specimen RC12 (see Figure 15). On the other hand, yielding load and ultimate load of UHTCC15 were about 15% higher than those of RC12, and ductility of UHTCC15 was better. It can be concluded that such thin UHTCC layer can obviously improve flexural performance of members, but cannot guarantee durability of the members. Considering both UHTCC25 and UHTCC15, UHTCC layer should overlaid longitudinal reinforcement in practical structures or members to avoid durability problems.

Illustrations of crack width developing with increase of applied load for RC12 reference beams and each group of UHTCC-FGC beams have been shown in Figures 16−20. From these pictures, it is found that there is a significant difference in crack opening behavior between RC12 beams and UHTCC-FGC beams. UHTCC25 will not be discussed in consideration of durability. The load level or deflection is indicated at the bottom of each picture, and corresponding crack width is shown in bracket.

Figure 15 Crack pattern of UHTCC15 at failure.

For the reference specimen RC12, the crack width measurement instrument indicated a continuously increasing crack width as the test progressed. Crack width of RC12 beams reached 0.12 mm when the applied load approached 60% of the yielding load, which exceeded the allowable crack width for ordinary reinforced concrete members under the worst exposed circumstances in Chinese code CCES 01-2004 "Guide to Durability Design and Construction of Concrete Structures" (0.10 mm)[22]. Crack width was approximately equal to 0.16 mm when applied load reached 74% of the yielding load. A total number of five cracks developed in the RC12 beam inside the gage zone. After yielding, the maximum crack width reached 0.28 mm. It is known from Chinese code GBJ50010-2002 "Code for Design of Concrete Structures"[25] that any crack widths larger than the limitation 0.3 mm (or 0.4 mm) may result in a high rate of reinforcement corrosion when the beam is to be exposed to room environment. A possible overload of reinforced concrete member may drive eventual durability problems.

For a given applied load level, crack width within UHTCC-FGC beams was always much smaller than that within RC12 beams. Figure 17 presents the development of crack width in UHTCC50 specimen, for which the cross section UHTCC layer had the same centroid with steel reinforcement. As the specimen was being loaded, the crack width measurement instrument indicated a slowly increasing crack width in UHTCC layer com

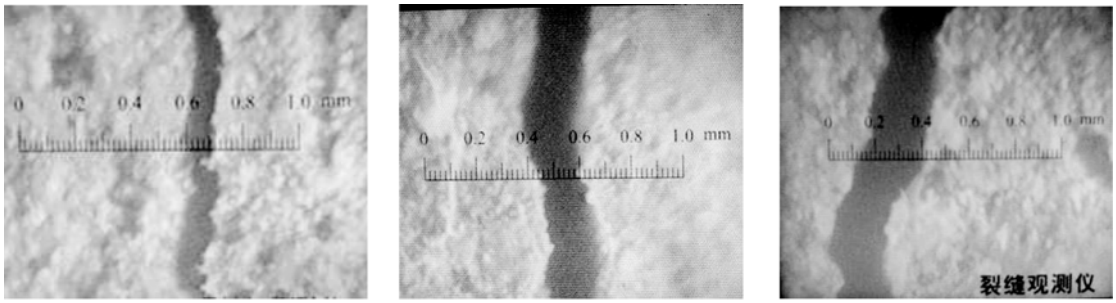

5.3 kN (0.12 mm) 6.6 kN (0.16 mm) Deflection reaches 15 mm after yielding (0.28 mm)

Figure 16 Development of the crack width in RC12.

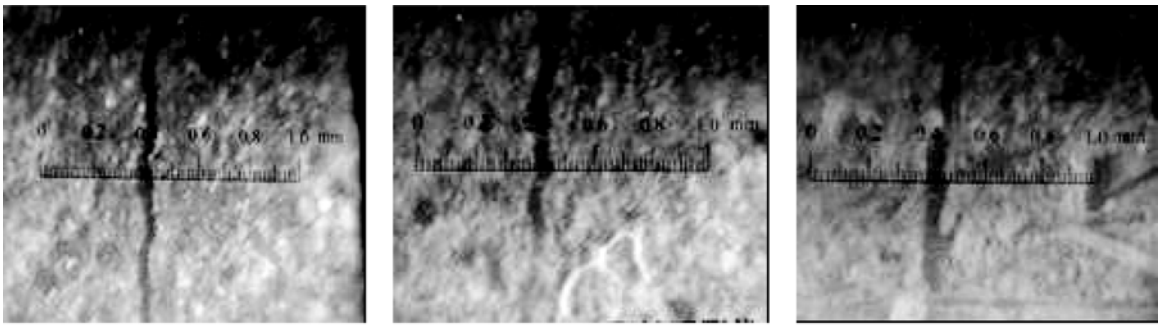

6 kN (0.04 mm) 8.2 kN (0.05 mm) 10 kN (0.05 mm)

Figure 17 Development of the crack width in UHTCC50.

pared with the reference specimens. When applied load reached approximately 60%—80% of the yielding load, crack width in UHTCC protection layer maintained about 0.04—0.05 mm. Even when the steel bar yielded, crack width in UHTCC material was still maintained at 0.05 mm. Investigation[8] indicated that the effect of self-healing of cement-based materials will close micro-cracks again. Furthermore, for general industrial and civil buildings, they can be supposed as structures without cracks if crack width is less than 0.05 mm[32]. For UHTCC-FGC beams with UHTCC material using as a replacement for the concrete that surrounded the longitudinal reinforcement, the development of crack width in UHTCC layer was at a very slow rate because of the appearance of new cracks, and the number of cracks in concrete layer was much more than in reference beams RC12. After yielding, the number of cracks in UHTCC50 beams still increased, which was different from RC12 beams. Comparing crack width between UHTCC layer and concrete layer, when the beams approached to their ultimate states (load reached 11.53 kN and deflection reached 37 mm), crack width in UHTCC layer was below 0.06 mm, while crack width in concrete layer was about 0.1 mm and it was far lower than that of RC12 beams (see Figure 18). Further imposed deformation was accommodated under the condition of larger crack number in UHTCC layer than in concrete layer. As above, crack width in UHTCC50 satisfied the requirement for Chinese code even when the structures were exposed to a possible overload. Durability of structures will be significantly improved by using UHTCC instead of concrete.

For UHTCC35 in which the UHTCC material just overlaid steel reinforcement, crack width maintained about 0.03—0.04 mm when the applied load reached 60%—80% of the yielding load. As the increase of applied load and deformation, a slowly increasing crack width in UHTCC layer was indicated in Figure 19. During the test, it is found that although the number of cracks in UHTCC35 was lower than that in UHTCC50, crack width of the two specimens were nearly the same and it was difficult to observe at ultimate state. It should be noted that load bearing capacity of UHTCC35 is close to that of UHTCC50, while the deformation capacity of the former reached 1.7 times of the latter by comparison. We can draw the conclusion that the thickness

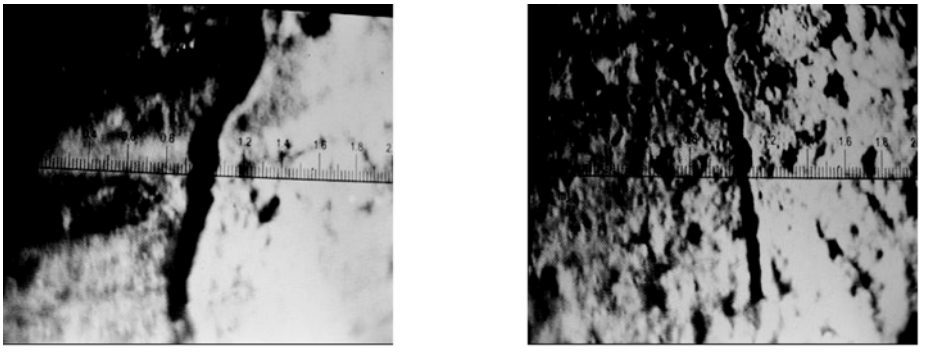

(a) Crack width in concrete layer (0.1 mm) (b) Crack width in UHTCC layer (0.05—0.06 mm)

Figure 18 Comparison of crack widths between concrete layer and UHTCC layer in UHTCC50 when the beams approached to their ultimate states (load reached 11.53 kN and deflection reached 37 mm).

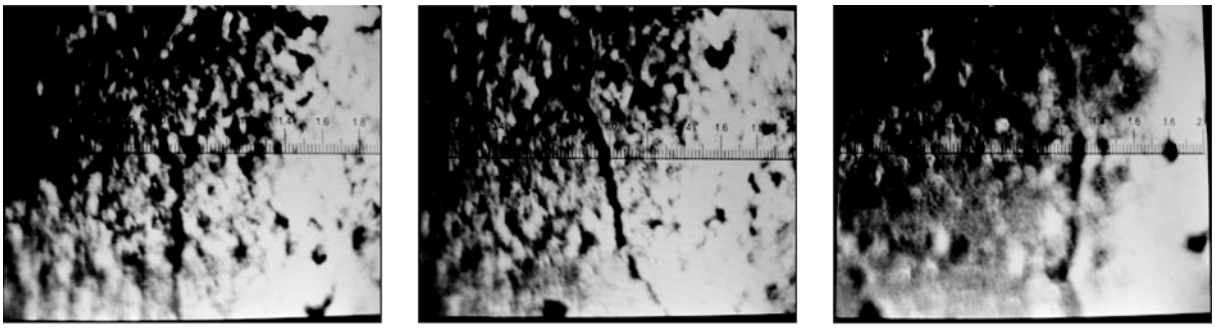

Figure 19 Development of the crack width in UHTCC35.

of UHTCC layer in UHTCC35, namely, the UHTCC material just overlays longitudinal reinforcement, is more appropriate to be utilized than that in UHTCC50 for which the cross section of UHTCC layer has the same centroid with reinforcement. Meanwhile, the UHTCC material can be saved by 40%.

In UHTCC15, UHTCC material of 15 mm thickness was used as protection cover and the longitudinal reinforcement was totally embedded in the concrete layer. Crack width in UHTCC15 reached 0.1 mm at yielding state (see Figure 20). It was a little higher compared with other groups of UHTCC-FGC beams, but lower than that of RC12 reference beams.

3 Determination of the optimal thickness of UHTCC layer

Given thickness of UHTCC layer t, Figure 21 shows the distribution of stress and strain along the beam depth at the ultimate state. To simplify calculation, the contribution of concrete in tension zone is not considered after cracking; tension stress of UHTCC after first-cracking is assumed to be σ_{tc} by neglecting the strain-hardening behavior. On the basis of superposition, we separate the compressive stress into two portions, one is contributed by UHTCC, and the other by tension steel reinforcement. Then the following equations can be obtained:

$$\int_c^h \sigma_c(x)b\mathrm{d}x = \int_c^h \sigma_{cI}(x)b\mathrm{d}x + \int_c^h \sigma_{cII}(x)b\mathrm{d}x = C_I + C_{II}, \tag{12}$$

$$tb\sigma_{tc}/f_y A_s = C_I / C_{II}. \tag{13}$$

For concrete composite beam strengthen with UHTCC, whose stress distribution corresponds with the left figure in Figure 21(c), the reinforcement of UHTCC is equivalent to that of the tension steel bar. Similar to the ordinary reinforced concrete beam, there are three possible failure modes for composite beam at the ultimate state. a) The first is compression failure mode characterized by concrete crushing failure, for composite beam with a thicker UHTCC layer. This condition is equivalent to heavily reinforced beam. b) The second is tension failure mode, which can be described by tension failure of UHTCC, for composite beam with a less thick UHTCC layer. This condition is equivalent to the under-reinforced beam. c) The last is tension-compression failure mode, which is characterized by concrete crushing failure and UHTCC tension failure at the same time. According to the calculation method of UHTCC-FGC beam, we have the following equations.

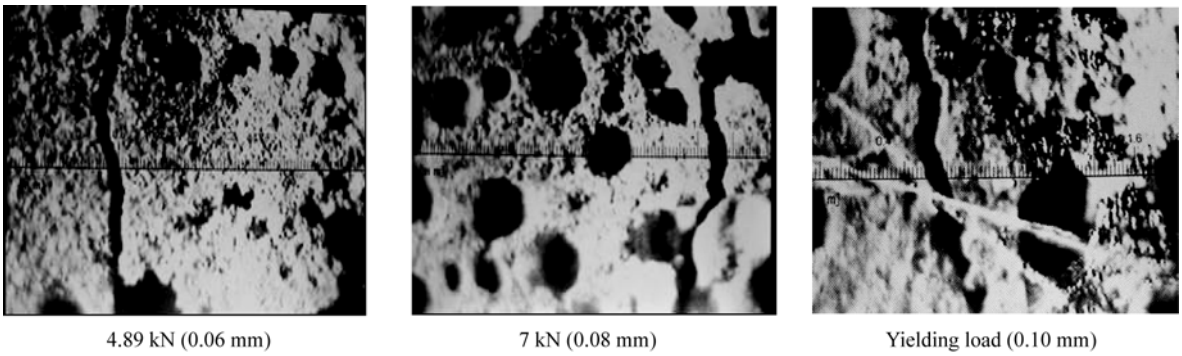

Figure 20 Development of the crack width in UHTCC15.

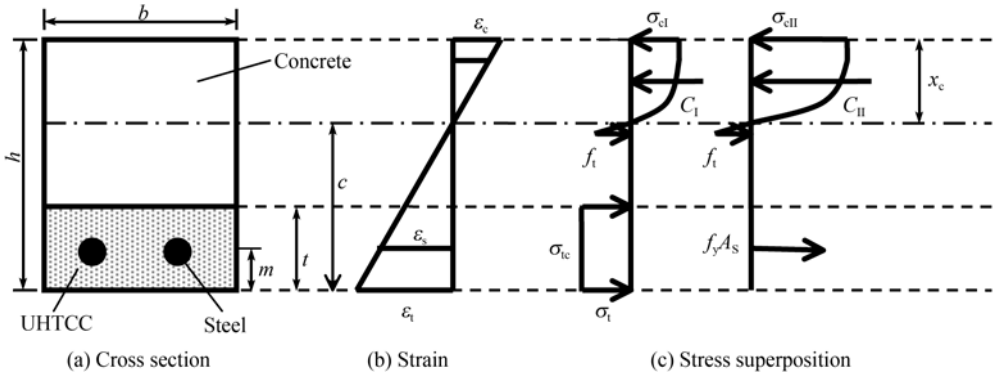

Figure 21 Distributions of stress and strain along beam depth of UHTCC-FGC beams at ultimate state.

When composite beam fails in the compression failure mode, the height of neutral axis can be expressed as

$$c = h - \frac{\frac{\sigma_{tc}}{f_{cI}}t}{1-\frac{\varepsilon_0}{3\varepsilon_{cu}}}. \tag{14}$$

When composite beam fails in the tension failure mode, the height of neutral axis can be expressed as

$$c = \frac{h-\frac{\sigma_{tc}}{f_{cI}}t}{\frac{\varepsilon_0}{3\varepsilon_{tu}}+1}. \tag{15}$$

Therefore, thickness of UHTCC layer for beams under the tension-compression failure mode is

$$t = \frac{f_{cI}\left(3\varepsilon_{cu}-\varepsilon_0\right)}{3\sigma_{tc}\left(\varepsilon_{cu}+\varepsilon_{tu}\right)}h. \tag{16}$$

According to eqs. (7) and (8), we have

$$\begin{cases} tb\sigma_{tc}/f_yA_s = f_{cI}/f_{cII}, \\ f_{cI}+f_{cII}=f_c. \end{cases} \tag{17}$$

Therefore,

$$f_{cI} = f_c\frac{tb\sigma_{tc}}{tb\sigma_{tc}+f_yA_s}. \tag{18}$$

Substituting eq. (18) into eq. (16), the critical thickness of UHTCC layer is

$$t_b = \frac{f_c\left(3\varepsilon_{cu}-\varepsilon_0\right)}{3\sigma_{tc}\left(\varepsilon_{cu}+\varepsilon_{tu}\right)}h - \frac{f_yA_s}{b\sigma_{tc}}. \tag{19}$$

For UHTCC-FGC beam with thickness of UHTCC layer $t<t_b$, it will fail in the tension failure mode because tensile strain of UHTCC reaches its ultimate value; when the thickness of UHTCC layer $t = t_b$, UHTCC-FGC beam will fail in the tension-compression failure mode; when the thickness of UHTCC layer $t>t_b$, UHTCC-FGC beam will fail in the compression failure mode. Considering durability of the beam, the thickness of UHTCC layer should be sufficient to ensure that the longitudinal reinforcement can be totally overlaid by UHTCC, namely

$$t > m + 0.5d_s, \tag{20}$$

where d_s denotes the diameter of tension steel. For the UHTCC-FGC beams discussed above, the critical thickness of UHTCC layer calculated through eq. (19) is 9.12 mm, while the UHTCC layer should be more than 32 mm via eq. (20). As a result, 35 mm was the optimal thickness in the test, providing both durability and economy.

4 Conclusions

The present work has investigated the bending behavior of UHTCC-FGC beam proposed on the basis of the concept of functional grade. Part of the concrete, which surrounds the main longitudinal reinforcement in a reinforced concrete flexural member, is strategically replaced with UHTCC material with excellent crack-onolling ability and high fracture resistance to improve durability of the reinforced concrete structure. After theoretical investigation, a four-point bending experiment was carried out to verify the proposed theoretical approach. The moment-curvature curves were measured and compared with the theoretical results. It is discovered that there is a reasonable agreement between them, especially that both moment and curvature present little difference before yielding. This suggests that the proposed theoretical model can be used to predict the load-deflection behavior of the UHTCC-FGC beams at

different stages. However, there is some difference between the calculated and the test deformations by reason of the neglect of slip between UHTCC and concrete and slip between steel and matrix. Moreover, the calculated ductility indices are safe and can be used to predict ductility of structures or members in practical design.

Compared with the reference reinforced concrete beams, the introduction of UHTCC material has not only significantly improved load bearing capacity and ductility, but also effectively controlled deformation of beam as well as reduced the use of steel reinforcements. Through theoretical analysis and the comparison among UHTCC-FGC beams with different thick UHTCC layers, the thickness of UHTCC layer which ensures UHTCC to just overlay the steel reinforcement was considered as the optimal thickness in this test. Specimens with the optimal thickness of UHTCC layer provides 30% higher load bearing capacity and 70% greater deformation ability than referenced RC specimens, and better flexural performance and less use of material than UHTCC-FGC specimens with thicker UHTCC layers. It is more worthy of note that with the use of UHTCC material in such an UHTCC-FGC flexural member, the opening of cracks can be greatly restricted and the crack width can be maintained below 0.05 mm before yielding. The possibility of corrosion can be evidently reduced in respect that the introduction of UHTCC can effectively control crack width so that durability will be improved markedly.

1 Li V C, Leung C K Y. Theory of steady state and multiple cracking of random discontinuous fiber reinforced brittle matrix composites. ASCE J Eng Mech, 1992, 118(11): 2246－2264
2 Li V C. From micromechanics to structural engineering—The design of cementitious composites for civil engineering applications. JSCE J Struct Mech Earthq Eng, 1993, 10(2): 37－48
3 Marshall D B, Cox B N. A J-integral method for calculating steady-state matrix cracking stresses in composites. Mech Mater, 1988(7): 127－133
4 Li V C. Engineered cementitious composites-tailored composites through micromechanical modeling. In: Banthia N, Bentur A, Mufti A, eds. Fiber Reinforced Concrete: Present and the Future. Montreal: Canadian Society for Civil Engineering, 1998. 64－97
5 Xu S L. Research on Ultrahigh Toughness Green ECC and its Application (in Chinese). Dalian: Dalian University of Technology, 2007
6 Li V C. On engineered cementitious composites (ECC)—a review of the material and its applications. J Adv Concr Technol, 2003, 1(3): 215－230
7 Li V C, Wang S, Wu C. Tensile strain-hardening behavior of PVA-ECC. ACI Mater J, 2001, 98(6): 483－492
8 Lepech M, Li V C. Durability and long term performance of engineered cementitious composites. In: Proceedings of Int'l Workshop on HPFRCC in Structural Applications. Honolulu: HPFRCC, 2005
9 Kuraray Co. Ltd. About PVA fibers: applications: structural. http://kuraray-am.com/ pvaf/ structural_case.php
10 Kojima S, Sakata N, Kanda T, et al. Application of direct sprayed ECC for retrofitting dam structure surface application for Mitaka-Dam. JCI Concr J, 2004, 42(5): 135－139
11 Japan Society of Civil Engineers. Recommendations for Design and Construction of High Performance Fiber Reinforced Cement Composite with Multiple Fine Cracks (in Japanese). HPFRCC, 2007
12 Rokogo K, Kanda T. Recent HPFRCC R&D Progress in Japan. In: Proceedings of Int'l Workshop on HPFRCC in Structural Applications. Honolulu: HPFRCC, 2005
13 Inaguma H, Seki M, Suda K, et al. Experimental study on crack-ridging ability of ECC for repair under train loading. In: Proceedings of Int'l Workshop on HPFRCC in Structural Applications. Honolulu: HPFRCC, 2005
14 Mitamura H, Sakata N, Suda K, et al. Application of overlay reinforcement method on steel deck utilizing engineered cementitious composites－Mihara Bridge. Bridge Found Eng, 2005, 39(8): 88－91
15 Maruta M, Kanda T, Nagai S, et al. New high-rise RC structure using pre-cast ECC coupling beam (in Japanese). Concrete J, 2005, 43(11): 18－26
16 Xu S L, Li Q H, Li H D. An experimental study on the flexural properties of carbon textile reinforced ECC (in Chinese). China Civ Eng J, 2007, 40(12): 69－76
17 Wu Z R, Li Y, Su H Z. Risk assessment method of major unsafe hydroelectric project. Sci China Ser E-Tech Sci, 2008, 51(9): 1345－1352
18 Yang F W, Zhang B J, Pan C C, et al. Sticky rice lime-mortar—one of the great inventions in ancient China. Sci China Ser E-Tech Sci, 2009, 52(6): 1641－1647
19 Maalej M, Li V C. Introduction of strain hardening engineered cementitious composites in design of reinforced concrete flexural members for improved durability. ACI Struct J, 1995, 92(2): 167－176
20 Maalej M, Ahmed S F U, Paramasivam P. Corrosion durability and structural response of functionally-graded concrete beams. In: JCI International Workshop on Ductile Fiber Reinforced Cementitious Composites (DFRCC)—Application and Evaluation. Takayama: DFRCC, 2002
21 Xu S L, Li Q H. Theoretical analysis on bending behavior of functionally graded composite beam crack-controlled by ultrahigh toughness cementitious composites. Sci China Ser E-Tech Sci, 2009, 52(2): 363－378
22 CCES01-2004 (revised edition). Design and Construction Direction to Concrete Structure Durability (in Chinese). Beijing: China Architecture & Building Press, 2005
23 Cheng W R, Kang G Y, Yan D H. Principle on Concrete Structure Design (in Chinese). Beijing: China Architecture & Building Press, 2002
24 Gergely P, Lutz L A. Maximum crack width in reinforced concrete flexural members. In: ACI-SP-20: Causes, Mechanism, and Control of Cracking in Concrete. Detroit: American Concrete Institute, 1968. 87－117
25 GB 50010-2002. Code for Design of Concrete Structures (in Chinese). Beijing: China Architecture & Building Press, 2002
26 Weimann M B, Li V C. Drying Shrinkage and Crack Width of ECC. Poland: BMC, 2003. 37－46
27 Lepech M, Li V C. Water permeability of cracked cementitious composites. In: Proceedings of Eleventh International Conference on Fracture. Turin: ICF, 2005
28 Takewaka K, Yamaguchi T, Maeda S. Simulation model for deterioration of concrete structures due to chloride attack. J Adv Concrete Tech, 2003, 1(2): 139－146
29 Wang K, Janse D C, Shah S P. Permeability study of cracked concrete, Cem Concrete Res, 1997, 27(3): 381－391
30 Maalej M, Li V C. Flexural strength of fiber cementitious composites. ASCE J Mater Civ Eng, 1994, 6(3): 390－406
31 Li V C, Horikoshi T, Ogawa A, et al. Micromechanics-based durability study of polyvinyl alcohol-engineered cementitious composite (PVA-ECC). ACI Mater J, 2004, 101(3): 242－248
32 Wang T M. Control of Cracking in Engineering Structure (in Chinese). Beijing: China Architecture and Building Press, 1997